

Research



Cite this article: Ezcurra MD, Butler RJ. 2018 The rise of the ruling reptiles and ecosystem recovery from the Permo-Triassic mass extinction. *Proc. R. Soc. B* **285**: 20180361. <http://dx.doi.org/10.1098/rspb.2018.0361>

Received: 15 February 2018

Accepted: 23 May 2018

Subject Category:

Palaeobiology

Subject Areas:

palaeontology, evolution

Keywords:

adaptive radiation, biotic crisis, morphological disparity, evolutionary rates, Diapsida, Archosauromorpha

Authors for correspondence:

Martín D. Ezcurra

e-mail: martindezcurra@yahoo.com.ar

Richard J. Butler

e-mail: r.butler.1@bham.ac.uk

Electronic supplementary material is available online at <https://doi.org/10.6084/m9.figshare.c.4116905>.

The rise of the ruling reptiles and ecosystem recovery from the Permo-Triassic mass extinction

Martín D. Ezcurra^{1,2} and Richard J. Butler²

¹Sección Paleontología de Vertebrados, CONICET-Museo Argentino de Ciencias Naturales, Ángel Gallardo 470, C1405DJR, Buenos Aires, Argentina

²School of Geography, Earth and Environmental Sciences, University of Birmingham, Edgbaston, Birmingham B15 2TT, UK

MDE, 0000-0002-6000-6450; RJB, 0000-0003-2136-7541

One of the key faunal transitions in Earth history occurred after the Permo-Triassic mass extinction (*ca* 252.2 Ma), when the previously obscure archosauromorphs (which include crocodylians, dinosaurs and birds) become the dominant terrestrial vertebrates. Here, we place all known middle Permian–early Late Triassic archosauromorph species into an explicit phylogenetic context, and quantify biodiversity change through this interval. Our results indicate the following sequence of diversification: a morphologically conservative and globally distributed post-extinction ‘disaster fauna’; a major but cryptic and poorly sampled phylogenetic diversification with significantly elevated evolutionary rates; and a marked increase in species counts, abundance, and disparity contemporaneous with global ecosystem stabilization some 5 million years after the extinction. This multiphase event transformed global ecosystems, with far-reaching consequences for Mesozoic and modern faunas.

1. Introduction

The devastating Permo-Triassic (PT) mass extinction (*ca* 252.2 Ma) dramatically impacted and remodelled global ecosystems [1–3]. On land, one of the key faunal transitions in Earth history took place during and following this extinction. The Palaeozoic amniote fauna, including synapsid groups such as anomodonts and gorgonopsians and parareptiles such as pareiasaurs, were decimated and largely displaced during the earliest Mesozoic by the previously obscure archosauromorphs [4,5]. Archosauromorphs, which include the ‘ruling reptiles’ or archosaurs (crocodylians, pterosaurs, dinosaurs, and their descendants, birds) and their close relatives, dominated terrestrial ecosystems for most of the Mesozoic and remain highly abundant and diverse in the modern biota [6–8].

Archosauromorphs originated during the middle–late Permian [9] and underwent a major radiation during the Triassic [6,10]. In the 20 million years following the PT mass extinction, species counts for archosauromorphs increased (greater than 100 valid species currently known) and the group achieved high morphological diversity, including highly specialized herbivores, large apex predators, marine predators, armoured crocodile-like forms, and gracile dinosaur precursors [6,10]. Despite this high diversity, scientific attention has mainly focused on the diversification of crown archosaurs (particularly bird-line archosaurs [6–8,10–13]), and the early diversification of archosauromorphs around the PT boundary has often been overlooked and little discussed (e.g. [14]). Thus, the patterns and processes of the ascendance of archosauromorphs to dominance by the Late Triassic are incompletely explored and poorly understood. Comprehensive macroevolutionary analysis of the dawn of the archosauromorph radiation has been hampered by the absence of a comprehensive, explicit phylogenetic framework for these early species.

Here, we quantitatively document major patterns of early archosauromorph biodiversity change, using a new phylogenetic dataset that includes for the first

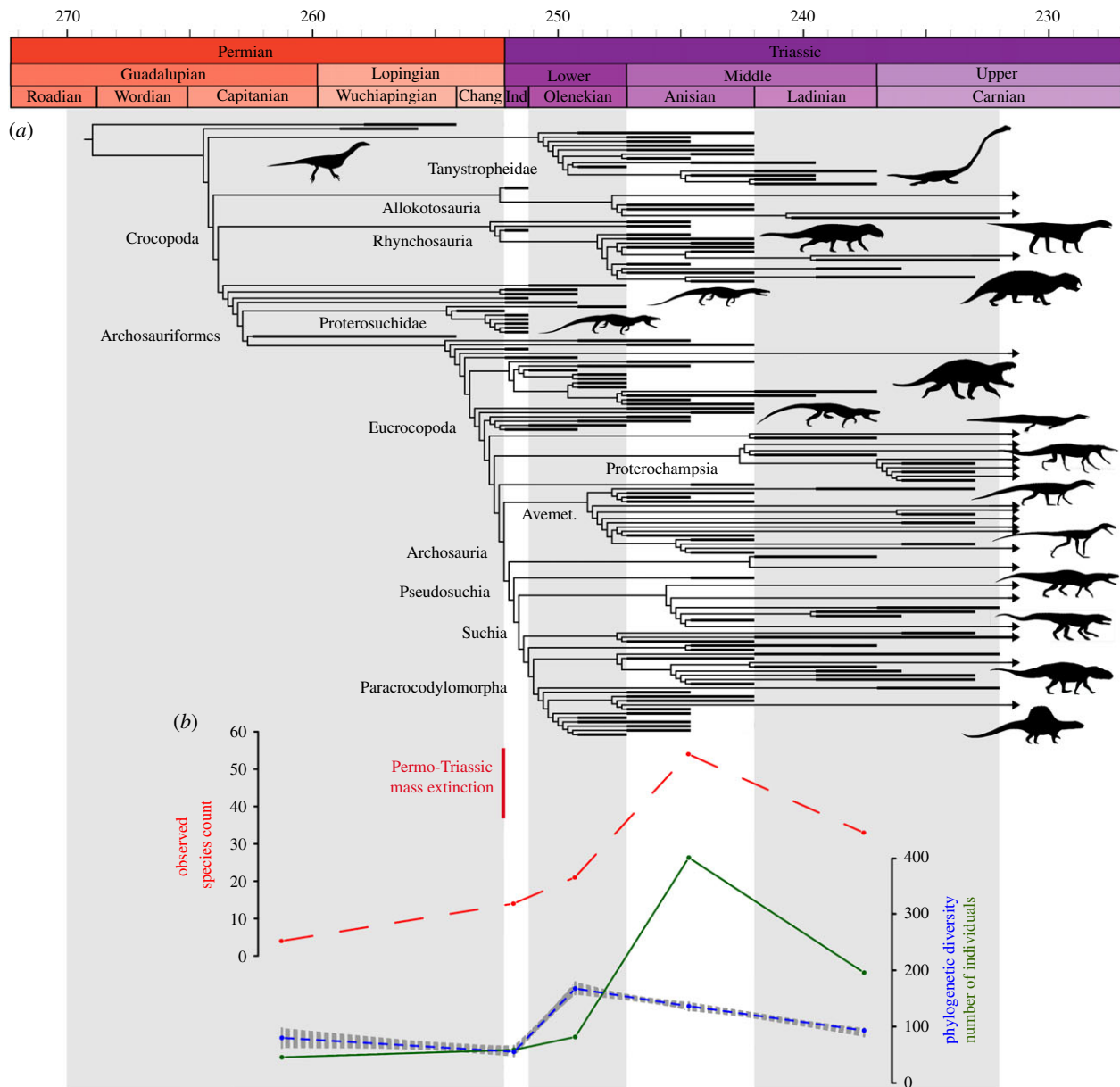


Figure 1. Diversity and abundance of late Permian–early Carnian archosauromorphs. (a) Randomly selected, time-calibrated most parsimonious tree (MPT) showing the phylogenetic diversity of early archosauromorphs. (b) Observed species count (dashed red line), phylogenetic diversity (values from 10 000 randomly selected MPTs as a dotted grey shadow and the mean of those values as a solid blue line), and number of individuals (solid green line without shadow) per time bin. Silhouette labels in electronic supplementary material, figure S11. Avemet., Avemetatarsalia. (Online version in colour.)

time all 108 currently valid middle Permian–early Late Triassic species (electronic supplementary material). Our analyses of morphological disparity, observed species counts, phylogenetic diversity and rates of phenotypic evolution are focused on the first 35 million years of archosauromorph evolution (*ca* 269–233 Ma) (figure 1*a*). These analyses aim to quantitatively explore one of the most important evolutionary radiations of vertebrates in the fossil record and the evolutionary patterns resulting from the reshaping and recovery of ecosystems in the aftermath of the deadliest mass extinction in Earth history.

2. Material and methods

(a) Taxon-character data matrix

The quantitative macroevolutionary analyses conducted here are based on the most comprehensive species-level phylogenetic dataset currently available for early archosauromorphs [10] and

its subsequent modifications (electronic supplementary material). We expanded this discrete morphological character matrix with the addition of 27 independent terminals (see electronic supplementary material, table S1), which resulted in a new dataset composed of 149 terminals and 688 characters. However, the full dimensions of this dataset are 689 characters and 151 terminals because character 119 was deactivated *a priori* and there are two additional taxonomic units representing the scorings of the complete hypodigms of *Archosaurus rossicus* (electronic supplementary material) and *Osmolskina czatkoviensis* (electronic supplementary material, table S1). These two terminals are not completely independent from the terminals representing the holotypes of these two species. In addition, some scorings were modified from previous versions of this dataset (electronic supplementary material).

(b) Phylogenetic analysis

Phylogenetic diversity and evolutionary rates calculations require explicit phylogenetic hypotheses [15,16]. As a result,

the complete data matrix including all 149 sampled terminals (including the complete hypodigm of *Osmolskina czatkoviensis*; electronic supplementary material, table S1) was analysed under equally weighted maximum parsimony using TNT 1.5 [17] in order to recover the required phylogenetic trees. The search strategy used a combination of the tree search algorithms Wagner trees, TBR branch swapping, sectorial searches, Ratchet (perturbation phase stopped after 20 substitutions), and Tree Fusing (5 rounds), and continued until the same minimum tree length was hit 100 times. The best trees obtained using this strategy were subjected to a final round of TBR branch swapping. Zero length branches in any of the recovered most parsimonious trees (MPTs) were collapsed and several characters were considered additive (electronic supplementary material).

(c) Time bins

The aim of our analyses is to explore the first 35 million years of the evolutionary history of Archosauromorpha, spanning the Permian origins of the group through to the appearance of archosauromorph-dominated ecosystems in the late Middle Triassic and earliest Late Triassic. We used five time bins in order to examine macroevolutionary patterns during this time span: middle–late Permian (approx. 17.1 Myr), Induan (1.0 Myr), Olenekian (4.0 Myr), Anisian (5.2 Myr) and Ladinian–early Carnian (approx. 9.0 Myr) [18]. Despite the very short length of the Induan, this stage was maintained as a separate time bin in order to capture diversity changes that occurred in the immediate aftermath of the PT mass extinction.

(d) Temporal calibration of trees

The evolutionary rates analyses require time-calibrated trees. The trees were calibrated with the `timePaleoPhy()` function of the package `paleotree` for R [19] using the ‘`mb1`’ calibration [11,20], a minimum branch length of 0.1 Myr, and a root age of 269.3 Ma based on the maximum bound estimated for the origin of Archosauromorpha [9] (figure 1a; electronic supplementary material, figure S4). Sensitivity analyses to explore the effect that different temporal calibrations may have on the results of the evolutionary rate analyses were conducted using ‘`mb1`’ calibrations with minimum branch lengths of 0.5 and 1.0 Myr, and also using the ‘`cal3`’ method [21] (electronic supplementary material).

(e) Morphological disparity analyses

Changes in morphological diversity (disparity) were quantified using the R package `Claddis` [16]. All non-archosauromorph species and archosauromorphs that occur in late Carnian or younger stratigraphic horizons were pruned before the disparity analyses, resulting in a final dataset of 112 terminals. Some terminals occur across two time bins because of uncertainty in the dating of the stratigraphic unit from which their fossils have been collected. These taxa were counted in both time bins in the disparity analyses (electronic supplementary material, tables S2 and S3). A sensitivity analysis pruning these terminals with stratigraphic uncertainty was conducted to evaluate the effect on the results (electronic supplementary material). Disparity curves were reconstructed using both generalized Euclidean distance (GED) and maximum observable rescaled distance (MORD) dissimilarity matrices (the two distance matrices recommended by Lloyd [16] for conducting disparity analyses based on discrete characters) generated from the taxon-character data matrix after the *a priori* pruning of non-archosauromorphs and those archosauromorph taxa stratigraphically younger than early Carnian (electronic supplementary material). These dissimilarity matrices were used to calculate weighted mean pairwise dissimilarity (WMPD) as a disparity

metric. Statistical significance between the disparity metrics for each time bin was assessed through 95% confidence intervals calculated from 1000 bootstrap replicates of the original taxon-character data matrix and a recalculation of the dissimilarity matrices and disparity metrics. Morphospace bivariate plots were generated for the entire dataset and each time bin based on the results of a principal coordinate analysis performed on the GED dissimilarity matrix. An additional disparity analysis using the same archosauromorph sampling as Foth *et al.* [14] was conducted using the same protocol.

(f) Phenotypic evolutionary rates analyses

Ancestral character-states were reconstructed with the package `Claddis` [16] using maximum likelihood in order to infer significant departures from equal rates of character evolution [22]. The phylogenetic analysis of the dataset compiled here recovered more than 10 000 MPTs. Therefore, in order to reduce computational time we used a random sample of 100 of these trees for the main evolutionary rate analyses (figure 2a). Non-archosauromorph terminals were pruned, but archosauromorph terminals stratigraphically younger than the early Carnian were retained because of the effects that the ghost lineages that they generate may have on older time bins (electronic supplementary material). All 100 subsampled trees were temporally calibrated using the protocol described above. The evolutionary rate analysis was conducted using the function `DiscreteCharacterRate()` {`Claddis`}, setting an alpha of 0.01 (electronic supplementary material, figure S8). An alpha of 0.01 was preferred because, as stated by Lloyd [16], there is generally a high heterogeneity of rates within datasets. A reduction in the alpha value therefore represents a conservative approach to reduce the number of significant values. Confidence intervals for each time bin were calculated using the function `plotMeanTimeseries()`, written by Close *et al.* [23], in order to test for the presence of significant rate differences in the early evolutionary history of Archosauromorpha (table 1). Sensitivity analyses using alternative tree calibrations were conducted using 10 trees for each ‘`mb1`’ calibration and the 60 trees generated by the ‘`cal3`’ method (electronic supplementary material).

(g) Time-series comparisons

Some of the macroevolutionary metrics calculated here may be correlated with one another and should not be considered as independent. To test this, we made statistical comparisons between observed species counts, phylogenetic diversity, specimen-level abundance data (i.e. number of individuals), and number of archosauromorph-bearing formations (as a metric of fossil record sampling). To compare these time series we used generalized least-squares regression (GLS) with a first order autoregressive model (`corARMA`) fitted to the data using the function `gls()` in the R package `nlme` v. 3.1–137 [24]. GLS reduces the chance of overestimating statistical significance of regression lines due to serial correlation. Time series were not log-transformed prior to analysis, as none were non-normally distributed (Shapiro–Wilk tests $p > 0.1$). We calculated likelihood-ratio based pseudo- R^2 values using the function `r.squaredLR()` of the R package `MuMIn` [25].

3. Results

Our results show a significant decrease in morphological disparity (using a MORD dissimilarity matrix, `MORDdm`) or a non-significant change (using a GED dissimilarity matrix, `GEDdm`) from the middle–late Permian to the earliest Triassic (Induan). Subsequently, a dramatic,

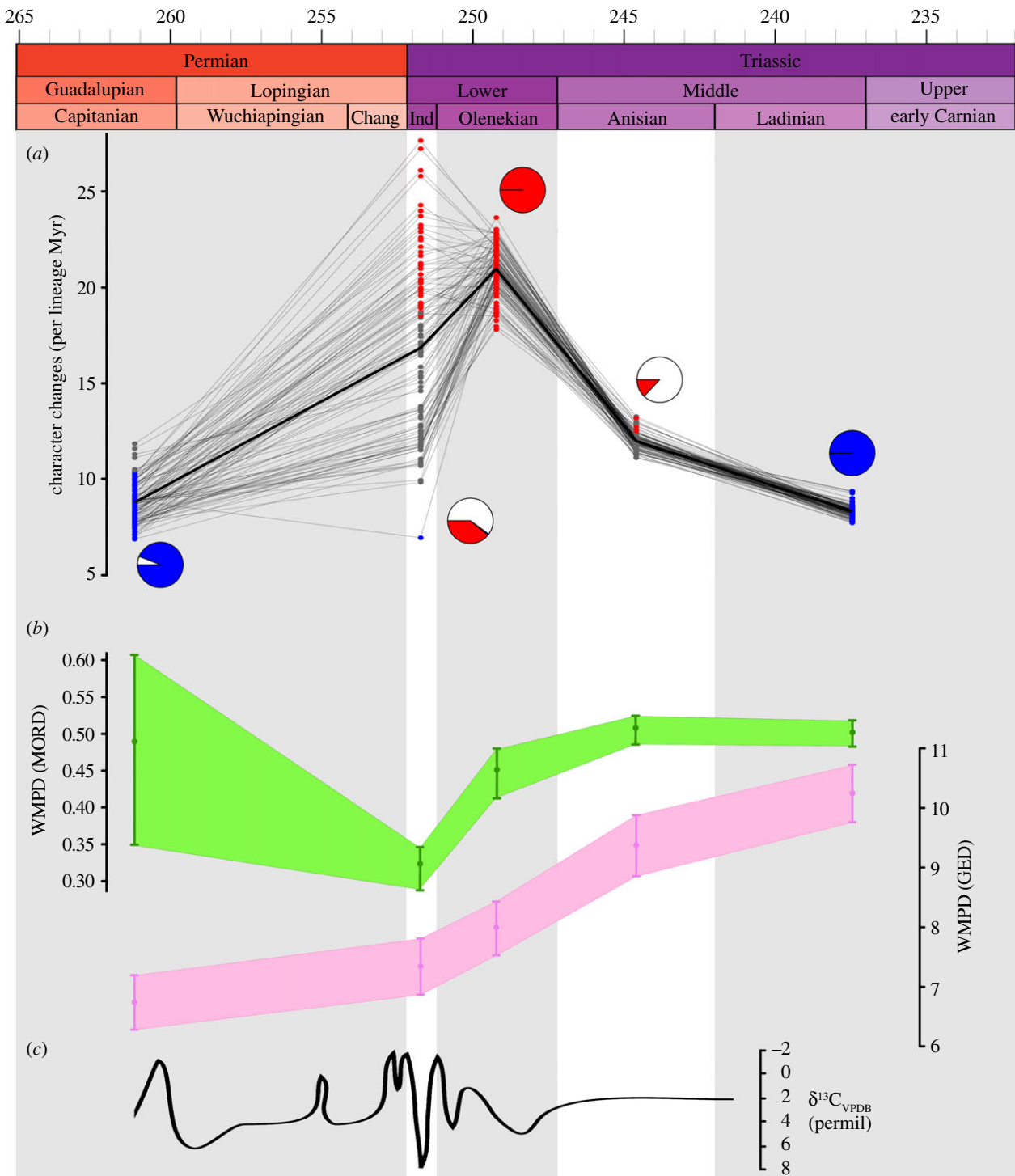


Figure 2. Evolutionary rates and morphological disparity of late Permian–early Carnian archosauromorphs. (a) ‘Spaghetti’ plot showing significantly fast (red) or slow (blue) rates of phenotypic evolution calculated from 100 randomly selected, time-calibrated MPTs. Grey points are non-significant values from the pooled average rate. Each thin line represents the analysis of one MPT. Pie charts show the ratio of significantly fast (red), slow (blue), and non-significant (white) rates at each time bin. (b) Morphological disparity of early archosauromorphs represented by weighted mean pairwise dissimilarity (WMPD) generated from GEDdm (green) and MORDdm (magenta), and its 95% confidence intervals generated using 1000 bootstrap replicates of the original data matrix. (c) Carbon isotope record from the late Capitanian to the earliest Ladinian (taken from [30]). (Online version in colour.)

significant increase occurs in the Olenekian (using MORDdm) or Anisian (using GEDdm) and high disparity levels are maintained in the Ladinian–early Carnian (figures 2b and 3; table 1). Evolutionary rates are significantly higher during the Olenekian—and in several topologies also during the Induan—than in other intervals (figure 2a and table 1), coincident with a peak in phylogenetic diversity (figure 1b). This peak in phylogenetic diversity results from a number of phylogenetically

deeply nested groups occurring in this interval, such as ctenosauriscids, which imply numerous ghost lineages [12] (figure 1a). Several of these lineages are identified as having significantly high evolutionary rates (e.g. electronic supplementary material, figure S8). By contrast, significantly lower evolutionary rates are recovered for the Ladinian–early Carnian in all analyses (figure 2a) and also during the middle–late Permian using ‘mbl’ calibrations (electronic supplementary material).

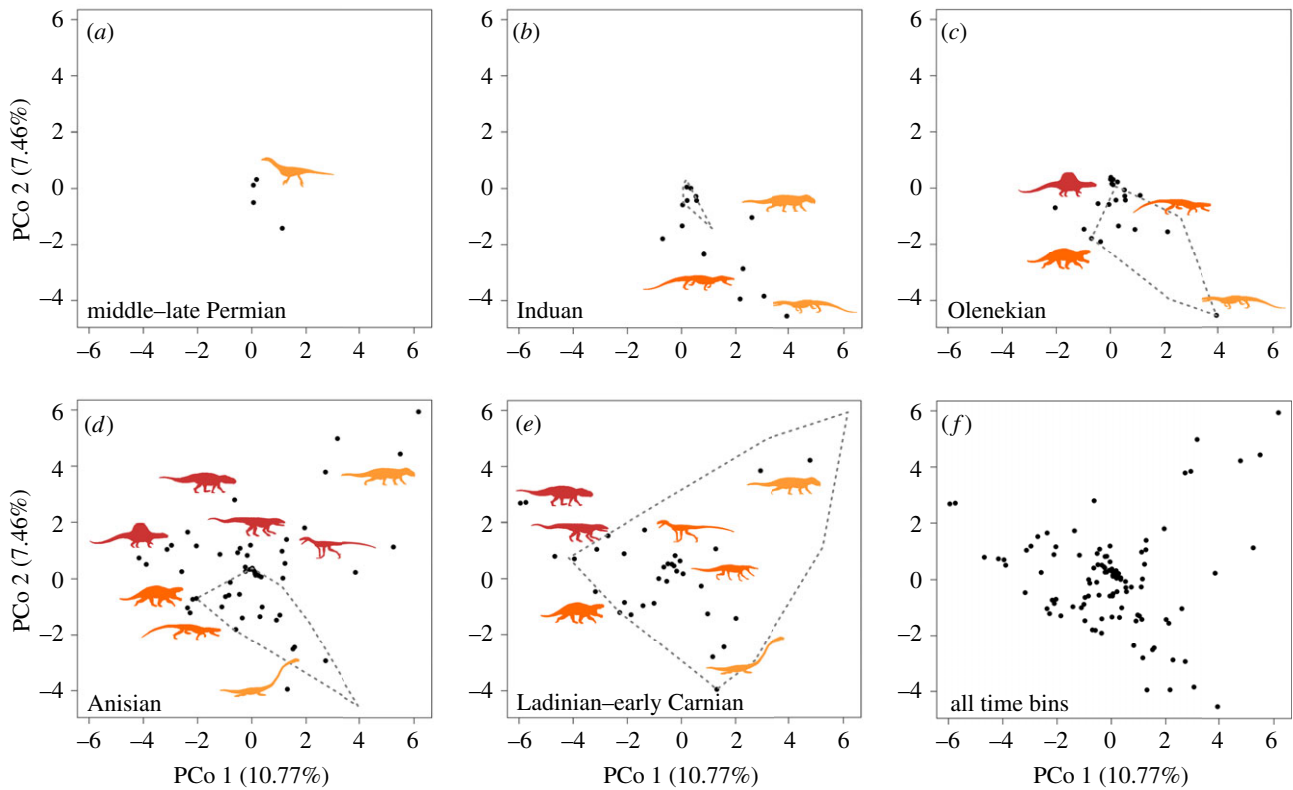


Figure 3. Morphospace occupation of late Permian–early Carnian archosauromorphs. (a–e) Sequence of morphospaces from the oldest to the youngest sampled time bin and (f) morphospace of all time bins together. Each plot shows the first two principal coordinate axes, which account for a summed variance of 18.23%. The black dots represent the position in the morphospace of each terminal in that time bin and the grey dotted line represents the convex hull of the morphospace of the previous time bin. The silhouettes show the approximate position of different main clades in the morphospace (silhouette labels in electronic supplementary material, figure S11). Highly fragmentary taxa tend to occupy a position closer to ($x = 0, y = 0$) in the ordination of the GED dissimilarity matrix, and thus the high density of taxa in this area is a methodological artefact (electronic supplementary material). (Online version in colour.)

Table 1. Results of the morphological disparity and evolutionary rates analyses. The disparity metrics were calculated using GEDdm and MORDdm and their 95% confidence intervals were calculated based on 1000 bootstrap replicates of the original data matrix. Reported phylogenetic diversity and evolutionary rates are mean values and their respective standard deviation. Evolutionary rate and weighted mean pairwise dissimilarity (WMPD) values that significantly differ from those of the previous time bin are given in italics. Car., Carnian; evol., Evolutionary; Lad., Ladinian; no. ind., number of individuals.

| time bin | no. ind. | phylogenetic diversity | WMPD (GED) | WMPD (MORD) | evol. rates |
|-----------------|----------|------------------------|----------------------|------------------------------|--------------|
| late Permian | 29 | 63.42 ± 5.79 | 6.74 (± 6.26–7.21) | 0.489 (± 0.349–0.607) | 8.76 ± 1.06 |
| Induan | 42 | 38.65 ± 2.95 | 7.35 (± 6.89–7.79) | <i>0.318 (± 0.288–0.346)</i> | 16.85 ± 4.52 |
| Olenekian | 65 | 150.91 ± 3.07 | 8.00 (± 7.54–8.43) | <i>0.445 (± 0.412–0.480)</i> | 20.97 ± 1.27 |
| Anisian | 383 | 119.52 ± 2.10 | 9.38 (± 8.86–9.86) | <i>0.505 (± 0.485–0.524)</i> | 11.97 ± 0.46 |
| Lad.-early Car. | 179 | 76.45 ± 1.77 | 10.25 (± 9.70–10.74) | 0.501 (± 0.482–0.519) | 8.27 ± 0.34 |

The observed or ‘raw’ species count of Induan archosauromorphs is at least double that recorded for the middle–late Permian, and observed species count increases only slightly during the Olenekian, but shows substantial increases into the Middle Triassic (figure 1b). Observed abundance data show a pattern consistent with that for observed species count, with only very slight increases through the middle–late Permian to Olenekian time span followed by a remarkable increase in the Anisian (figure 1b). However, the time series of observed species count, number of individuals, and geological sampling (numbers of rock units in which archosauromorphs occur) are not significantly different to each other ($p < 0.05$; pseudo- $R^2 > 0.85$), which might reflect

either a sampling bias or an increase of archosauromorph abundance in their ecosystems. Conversely, estimated phylogenetic diversity is not correlated with sampling estimates or abundance ($p > 0.15$; pseudo- $R^2 < 0.35$) (electronic supplementary material, table S6).

4. Discussion

Our analyses support a multiphase model of early archosauromorph diversification, largely in response to the events of the PT mass extinction. Archosauromorphs most likely originated in the middle Permian, and underwent a substantial phylogenetic diversification and dispersed across

Pangea [9,26]. However, disparity remained low, and low fossil abundance (figures 1*b*, 2*b* and 3*b,c*) suggests either that archosauromorphs remained very minor components of terrestrial ecosystems, or that this diversification took place in geographical regions or environments that remain poorly sampled. Many major lineages of archosauromorphs are inferred to have passed through the PT boundary and the group may have been comparatively little affected by the extinction event [10] (figure 1*a*). The Induan, immediately after the extinction, saw a substantial increase in archosauromorph abundance and a high observed species count relative to the length of the time bin, characterized by a low disparity (figure 2*b*), globally distributed archosauromorph 'disaster fauna' dominated by proterosuchids and a number of morphologically similar lineages (e.g. *Prolacerta*) [27] (figure 3*b*). This disaster fauna was apparently short-lived: in South Africa, *Proterosuchus* occurs only between 5 and 14 m above the PT boundary [28]. Similar patterns have been documented for the synapsid *Lystrosaurus* following the PT extinction [29], and earliest Triassic tetrapod assemblages on land appear in general to have been highly uneven and dominated by a few highly abundant or diverse taxa [30,31].

Major perturbations in the global carbon cycle, referred to as 'chaotic carbon cycling', have been documented through the Early Triassic (Induan and Olenekian) [32,33] (figure 2*c*). These perturbations have been suggested to reflect either successive short-term greenhouse crises and rapid environmental change or boom–bust cycles of ecosystem instability [30,33,34]. This interval of instability coincides with generally elevated global temperatures that would have limited diversity in equatorial regions and a well-known gap in the coal record that reflects lowered plant productivity and diversity [34,35]. Our data suggest that archosauromorphs underwent a major phylogenetic diversification in the Olenekian (1–5 million years [Myr] after the extinction), characterized by significantly elevated evolutionary rates (figure 2*a*), with the origins or initial diversification of major clades such as rhynchosaurs, archosaurs, erythrosuchids and tanystropheids (figure 1*a*). The fossil record shows that mass extinctions promote adaptive radiations in surviving, often previously marginal, clades because of the disappearance of species or entire lineages opening new vacancies in ecological space [36,37]. Thus, this general pattern suggests that the diversification of archosauromorphs was a response to vacant ecological space following the PT extinction, and the subsequent disappearance of the short-lived post-PT disaster fauna. However, observed species count and abundance remained low in the Olenekian, and similar to those of the Induan (figures 1*b*, 2*b* and 3*b,c*). As such, this major phylogenetic and probable morphological diversification in the Olenekian is at present largely cryptic and very incompletely sampled, potentially reflecting the very low abundances of individual archosauromorph species in the highly uneven and unstable Early Triassic ecosystems (figure 1*b*), as well as the limited geographical range over which known Olenekian tetrapod fossils occur [35].

The Anisian (5–10 Myr after the extinction) is characterized by marked increases in observed species count, abundance and disparity among archosauromorphs (figures 1*b*, 2*b* and 3*d*), as

well as substantial increases in maximum body size [38]. An increased ecomorphological disparity during the Anisian matches previous results based on geometric morphometrics of archosauromorph skulls [14] (electronic supplementary material) and is documented in the skeletal fossil record by the appearance of large hypercarnivores, bizarre and highly specialized herbivores, long-necked marine predators, and gracile and agile dinosauromorphs [6,10]. This coincides with the end of the interval of intense carbon perturbations, a global cooling event, and the return of conifer-dominated forests [34], suggesting the recovery and stabilization of global ecosystems [30]. This stabilization may have acted as an extrinsic factor that promoted increases in abundance among archosauromorph lineages as community evenness recovered, with a previously largely cryptic diversification becoming better sampled in the fossil record as a result. Similar patterns are observed among marine tetrapods, with the first sauropterygians and ichthyosauromorphs being documented close to the Olenekian–Anisian boundary [39], but likely reflecting a temporally somewhat deeper period of currently unsampled phylogenetic diversification [40].

Our analyses of archosauromorph biodiversity change around the PT boundary support a diversity-first model of evolution, in which a rapid speciation of similar disaster taxa filled ecospace, followed by more steady adaptive evolution into new sectors of morphospace as ecosystems and community interactions stabilized (figure 3) [3]. A similar evolutionary pattern has been reported among dicynodonts in terrestrial ecosystems in the aftermath of the PT mass extinction [41], and has also been documented in fossil marine animals [42], including graptoloids [43] and ammonoids [44] during the Ordovician and PT biotic crises, respectively. More detailed work on other taxonomic groups is needed to establish if this pattern characterizes other terrestrial clades and extinction events.

The establishment of high abundance, ecomorphological diversity, and observed species counts and phylogenetic diversity of archosauromorphs by the Middle Triassic paved the way for the ongoing diversification of the group (including the origins of dinosaurs, crocodylomorphs, and pterosaurs) in the Late Triassic, and their dominance of terrestrial ecosystems for the next 170 million years. Our results show the fundamental role of the PT mass extinction and its aftermath in reshaping terrestrial ecosystems, and its far-reaching impact on the faunas of the Mesozoic and modern world.

Data accessibility. Species occurrence data, R scripts, data matrices and tree files are available as online electronic supplementary material.

Authors' contributions. M.D.E. and R.J.B. designed the research project, conducted the analyses and contributed to the text of the manuscript; M.D.E. scored most terminals and made the figures.

Competing interests. We declare we have no competing interests.

Funding. This research was supported by the DFG Emmy Noether Programme (BU 2587/3-1 to R.J.B.), a Marie Curie Career Integration Grant (630123 ARCHOSAUR RISE to R.J.B.), and a National Geographic Society Young Explorers Grant (9467-14 to M.D.E.).

Acknowledgements. We thank Roger Close and David Button for their comments and help with some of the analyses. We also thank the Associate Editor Erin Saupe, Stephen Brusatte, and an anonymous reviewer for their comments, which improved the manuscript.

References

- Raup DM. 1979 Size of the Permo-Triassic bottleneck and its evolutionary implications. *Science* **206**, 217–218. (doi:10.1126/science.206.4415.217)
- Erwin DH. 1994 The Permo-Triassic extinction. *Nature* **367**, 231–236. (doi:10.1038/367231a0)
- Chen Z-Q, Benton MJ. 2012 The timing and pattern of biotic recovery following the end-Permian mass extinction. *Nat. Geosci.* **5**, 375–383. (doi:10.1038/ngeo1475)
- Bakker RT. 1977 Tetrapod mass extinctions—a model of the regulation of speciation rates and immigration by cycles of topographic diversity. In *Patterns of evolution as illustrated by the fossil record* (ed. A Hallan), pp. 439–468. New York, NY: Elsevier.
- Benton MJ, Tverdokhlebov VP, Surkov MV. 2004 Ecosystem remodelling among vertebrates at the Permo-Triassic boundary in Russia. *Nature* **432**, 97–100. (doi:10.1038/nature02950)
- Nesbitt SJ. 2011 The early evolution of archosaurs: relationships and the origin of major clades. *Bull. Am. Mus. Nat. Hist.* **352**, 1–292. (doi:10.1206/352.1)
- Brusatte SL, Nesbitt SJ, Irmis RB, Butler RJ, Benton MJ, Norell MA. 2010 The origin and early radiation of dinosaurs. *Earth Sci. Rev.* **101**, 68–100. (doi:10.1016/j.earscirev.2010.04.001)
- Langer MC, Ezcurra MD, Bittencourt J, Novas FE. 2010 The origin and early evolution of dinosaurs. *Biol. Rev.* **85**, 55–110. (doi:10.1111/j.1469-185X.2009.00094.x)
- Ezcurra MD, Scheyer TM, Butler RJ. 2014 The origin and early evolution of Sauria: reassessing the Permian saurian fossil record and the timing of the crocodile-lizard divergence. *PLoS ONE* **9**, e89165. (doi:10.1371/journal.pone.0089165)
- Ezcurra MD. 2016 The phylogenetic relationships of basal archosauromorphs, with an emphasis on the systematic of proterosuchian archosauriforms. *PeerJ* **4**, e1778. (doi:10.7717/peerj.1778)
- Brusatte SL, Benton MJ, Ruta M, Lloyd GT. 2008 Superiority, competition and opportunism in the evolutionary radiation of dinosaurs. *Science* **321**, 1485–1488. (doi:10.1126/science.1161833)
- Butler RJ, Brusatte SL, Reich M, Nesbitt SJ, Schuch RR, Hornung JJ. 2011 The sail-backed reptile *Ctenosauriscus* from the latest Early Triassic of Germany and the timing and biogeography of the early archosaur radiation. *PLoS ONE* **6**, e25693. (doi:10.1371/journal.pone.0025693)
- Nesbitt SJ *et al.* 2017 The earliest bird-line archosaurs and the assembly of the dinosaur body plan. *Nature* **544**, 484–487. (doi:10.1038/nature22037)
- Foth C, Ezcurra MD, Sookias R, Brusatte SL, Butler RJ. 2016 Unappreciated diversification of stem archosaurs during the Middle Triassic predated the dominance of dinosaurs. *BMC Evol. Biol.* **16**, 188. (doi:10.1186/s12862-016-0761-6)
- Norell MA. 1992 Taxic origin and temporal diversity: the effect of phylogeny. In *Extinction and phylogeny* (eds MJ Novacek, QD Wheeler), pp. 88–118. New York, NY: Columbia University Press.
- Lloyd GT. 2016 Estimating morphological diversity and tempo with discrete character–taxon matrices: implementation, challenges, progress, and future directions. *Biol. J. Linn. Soc.* **118**, 131–151. (doi:10.1111/bij.12746)
- Goloboff PA, Catalano SA. 2016 TNT version 1.5, including a full implementation of phylogenetic morphometrics. *Cladistics* **32**, 221–238. (doi:10.1111/cla.12160)
- Gradstein FM, Ogg JG, Schmitz MD, Ogg G. 2012 *The geologic time scale 2012*, vol. 2. Boston, MA: Elsevier.
- Bapst DW. 2012 paleotree: An R package for paleontological and phylogenetic analyses of evolution. *Meth. Ecol. Evol.* **3**, 803–807. (doi:10.1111/j.2041-210X.2012.00223.x)
- Laurin M. 2004 The evolution of body size, Cope's Rule and the origin of amniotes. *Syst. Biol.* **53**, 594–622. (doi:10.1080/10635150490445706)
- Bapst DW. 2013 A stochastic rate-calibrated method for time-scaling phylogenies of fossil taxa. *Meth. Ecol. Evol.* **4**, 724–733. (doi:10.1111/2041-210X.12081)
- Lloyd GT, Wang SC, Brusatte SL. 2012 Identifying heterogeneity in rates of morphological evolution: discrete character change in the evolution of lungfish (Sarcopterygii: Dipnoi). *Evol.* **66**, 330–348. (doi:10.1111/j.1558-5646.2011.01460.x)
- Close RA, Friedman M, Lloyd GT, Benson RB. 2015 Evidence for a mid-Jurassic adaptive radiation in mammals. *Curr. Biol.* **25**, 2137–2142. (doi:10.1016/j.cub.2015.06.047)
- Pinheiro J, Bates D, DebRoy S, Sarkar D, R Core Team. 2018 nlme: Linear and nonlinear mixed effects models. R package version 3.1-137. See <https://CRAN.R-project.org/package=nlme>.
- Bartoń K. 2018 MuMIn: multi-model inference. R package version 1.40.4. See <http://cran.r-project.org/package=MuMIn>
- Bernardi M, Klein H, Petti FM, Ezcurra MD. 2015 The origin and early radiation of archosauriforms: integrating the skeletal and footprint record. *PLoS ONE* **10**, e0128449.
- Ezcurra MD, Butler RJ. 2015 Taxonomy of the proterosuchid archosauriforms (Diapsida: Archosauromorpha) from the earliest Triassic of South Africa, and implications for the early archosauriform radiation. *Palaentology* **58**, 141–170. (doi:10.1111/pala.12130)
- Smith RMH, Botha-Brink J. 2014 Anatomy of a mass extinction: sedimentological and taphonomic evidence for drought-induced die-offs at the Permo-Triassic boundary in the main Karoo Basin, South Africa. *Palaogeogr. Palaeoclimatol. Palaeoecol.* **396**, 99–118. (doi:10.1016/j.palaeo.2014.01.002)
- Botha J, Smith RMH. 2006 Rapid vertebrate recuperation in the Karoo Basin of South Africa following the end-Permian extinction. *J. Afr. Earth Sci.* **45**, 502–514. (doi:10.1016/j.jafrearsci.2006.04.006)
- Irmis RB, Whiteside JH. 2011 Delayed recovery of non-marine tetrapods after the end-Permian mass extinction tracks global carbon cycle. *Proc. R. Soc. B* **279**, 1310–1318. (doi:10.1098/rspb.2011.1895)
- Button DJ, Lloyd GT, Ezcurra MD, Butler RJ. 2017 Mass extinctions drove global faunal cosmopolitanism on the supercontinent Pangaea. *Nat. Commun.* **8**, 733. (doi:10.1038/s41467-017-00827-7)
- Payne JL, Lehmann DJ, Wei J, Orchard MJ, Schrag DP, Knoll AH. 2004 Large perturbations of the carbon cycle during recovery from the end-Permian extinction. *Science* **305**, 506–509. (doi:10.1126/science.1097023)
- Whiteside JH, Ward PD. 2011 Ammonoid diversity and disparity track episodes of chaotic carbon cycling during the early Mesozoic. *Geology* **39**, 99–102. (doi:10.1130/G31401.1)
- Sun Y, Joachimski MM, Wignall PB, Yan C, Chen Y, Jiang H, Wang L, Lai X. 2012 Lethally hot temperatures during the Early Triassic greenhouse. *Science* **338**, 366–370. (doi:10.1126/science.1224126)
- Bernardi M, Petti FM, Benton MJ. 2018 Tetrapod distribution and temperature rise during the Permian-Triassic mass extinction. *Proc. R. Soc. B* **285**, 20172331. (doi:10.1098/rspb.2017.2331)
- Schluter D. 2000 *The ecology of adaptive radiation*. Oxford, UK: Oxford University Press.
- Yoder JB *et al.* 2010 Ecological opportunity and the origin of adaptive radiations. *J. Evol. Biol.* **23**, 1581–1596. (doi:10.1111/j.1420-9101.2010.02029.x)
- Sookias RB, Butler RJ, Benson RB. 2012 Rise of dinosaurs reveals major body-size transitions are driven by passive processes of trait evolution. *Proc. R. Soc. B* **279**, 2180–2187. (doi:10.1098/rspb.2011.2441)
- Motani R, Jiang DY, Chen GB, Tintori A, Rieppel O, Ji C, Huang JD. 2015 A basal ichthyosauriform with a short snout from the Lower Triassic of China. *Nature* **517**, 485–488. (doi:10.1038/nature13866)
- Motani R, Jiang DY, Tintori A, Ji C, Huang JD. 2017 Pre- versus post-mass extinction divergence of Mesozoic marine reptiles dictated by time-scale dependence of evolutionary rates. *Proc. R. Soc. B* **284**, 20170241. (doi:10.1098/rspb.2017.0241)
- Ruta M, Angielczyk KD, Fröbisch J, Benton MJ. 2013 Decoupling of morphological disparity and taxic diversity during the adaptive radiation of anomodont therapsids. *Proc. R. Soc. B* **280**, 20131071. (doi:10.1098/rspb.2013.1071)
- Sepkoski Jr JJ. 1998 Rates of speciation in the fossil record. *Phil. Trans. R. Soc. Lond. B* **353**, 315–326. (doi:10.1098/rstb.1998.0212)
- Bapst DW, Bullock PC, Melchin MJ, Sheets HD, Mitchell CE. 2012 Graptoloid diversity and disparity became decoupled during the Ordovician mass extinction. *Proc. Natl Acad. Sci USA* **109**, 3428–3433. (doi:10.1073/pnas.1113870109)
- McGowan AJ. 2004 The effect of the Permo-Triassic bottleneck on Triassic ammonoid morphological evolution. *Paleobiology* **30**, 369–395. (doi:10.1666/0094-8373(2004)030<0369:TEOTPB>2.0.CO;2)